Planetary and Space Science 215 (2022) 105463

Contents lists available at ScienceDirect

Planetary and Space Science

journal homepage: www.elsevier.com/locate/pss

ECOCEL database: An online tool for asteroid mission planning

Irina Kovalenko [a,*], Jean Kempf [a], Oksana Popovichenko [a,b], Thibault Gateau [a], Stéphanie Lizy-Destrez [a]

[a] ISAE-SUPAERO, 10 av. Edouard Belin, 31400, Toulouse, France
[b] National Aerospace University, 17, Chkalova str., 61070, Kharkiv, Ukraine

ARTICLE INFO

Keywords:
Near-Earth asteroids
Asteroid resource exploitation
Mission analysis
Asteroid database

ABSTRACT

The Near-Earth asteroids (NEAs) may be the most promising targets for resources to be used for space manufacturing. Metals, semiconductors and volatiles from asteroids can be used for production of propellant, space constructions and life-support of crewed missions. An assessment of accessible resources and selection of best asteroids-candidates implies a mission analysis together with a compositional data. The ECOCEL database is a web-based tool developed at ISAE-SUPAERO for selection of asteroids-candidates for future space mining missions. The database contains 326 NEAs. For each object, the database includes (i) one-way and round-trip rendezvous mission opportunities computed for 2025–2050 launch period, and (ii) estimated composition inferred from spectral classification and meteorite analogs. The web-application enables searching for suitable target asteroids while specifying mission constraints. In addition, the ECOCEL tool provides a visualisation of compositional data for the entire sample of asteroids.

1. Introduction

Asteroid materials may provide valuable resources for the future space manufacturing. In recent years, this concept has been studied for technological and economical viability to support the developing space infrastructure of deep-space and cislunar missions (Oleary et al., 1979; Jedicke et al., 2018; Probst et al., 2020). In particular, the near-Earth asteroids (NEAs), containing metals and volatiles, may be the most accessible resources to be used for space constructions, life support systems and propellant (Ross, 2001). In addition, volatile rich objects are of scientific interest, containing a key information about the evolution of the Solar System.

Within this context the multidisciplinary project ECOCEL (stands for "Exploitation des Ressources des Corps Célestes", in French) conducts study on exploration and commercial exploitation of celestial bodies. The objective of the project is to provide an overview and recommendations about the potential of the space mining industry.

The selection of candidate asteroids for resource exploration lies in two important criteria: composition and accessibility. The compositional information defines possible resources for the mining, or *in situ* production. The second factor, accessibility of targets, is commonly measured in delta-V, the required velocity changes expressed in km/s. Depending on mission scenario, the assessment of delta-V may include optimal delta-V solutions for both the outbound and return transfers, and also a delta-V for a bounded Earth orbit of departure or final capture. First order estimations in various studies (Binzel et al., 2004; Elvis et al., 2011; Yárnoz et al., 2013) show that the vast majority of NEAs are favorable for resource exploitation, and even, accessible for human exploration missions (Zimmerman et al., 2010).

The best method to study asteroid composition is the *in situ* exploration. To date, only four space missions have landed on NEAs: NASA's Near-Shoemaker and OSIRIS-REx, and JAXA's Hayabusa and Hayabusa2 (see, e.g., Veverka et al., 2001; Lauretta et al., 2017; Fujiwara et al., 2006; Tsuda et al., 2020). Bringing remarkable scientific results, spacecraft missions to asteroids require however a very high technological and financial contribution. To study the large population of NEAs by more affordable means, the compositional estimation can be done using available on Earth samples of meteorites and spectral characteristics of asteroids from observations by telescopes (Cloutis et al., 2014). The observed spectral properties of NEAs are available from several projects, such as NEOSHIELD-2 (Perna et al., 2018), MANOS (Devogèle et al., 2019), and MITHNEOS (Binzel et al., 2019). This last survey collected and analyzed the spectra for more than 1000 NEOs.

Webster (2013) developed Asterank database, evaluating the economic prospects of mining over 600,000 asteroids. The database was created by using publicly available data and scientific papers. The majority of

* Corresponding author.
E-mail address: irina.kovalenko@isae-supaero.fr (I. Kovalenko).

https://doi.org/10.1016/j.pss.2022.105463
Received 17 November 2021; Received in revised form 21 February 2022; Accepted 14 March 2022

asteroids in the database have no spectral classification, and consequently an accurate estimation of the cost of mining and composition are not available. The NHATS (Near-Earth Object Human Space Flight Accessible Targets Study) group maintains a database (NHATS, 2021) of asteroids that may be well-suited to future human space flight round-trip missions. This database also contains future observing opportunities of potential mission targets. However, spectral types or estimated composition are not provided. Another JPL maintained database, computed by Lance A. M. Benner, provides rendezvous delta-V for 26193 asteroids. This database is not constrained by human flight mission criteria, but doesn't include information about spectral classification or composition.

The ECOCEL database tool ecocel-database.com was designed for an assessment of available resources of asteroids. In addition to existing databases, the ECOCEL tool takes into account both: mission opportunities and compositional estimation. The mission analysis was computed for one-way and round-trip rendezvous missions. The estimation of composition was inferred from spectral classification and meteorite links. Furthermore, the ECOCEL web-application contains a data visualisation tools, allowing user to make a data analysis from the set of asteroids.

This paper is organised as follows. First, the data set of considered asteroids is presented. Then, the estimation of composition of asteroids is described in Section 3. The description of the database with computed launch opportunities between 2030 and 2050 is given in Section 4. The interface of the ECOCEL web-application is presented in Section 5. The main conclusion is summarised in Section 6.

2. Considered asteroids

Currently, there are over 20000 known NEAs (NASA, 2020). In this work, the main information about asteroids, including physical and orbital characteristics, is adopted from the JPL Small-Body Database (Chamberlin et al., 2020). The ECOCEL database tool contains a subset of NEAs with defined spectral types, resulting in a sample of 326 asteroids from the JPL Small-Body Database. Two spectral classifications are available: Tholen (Tholen) and SMASSII (Bus and Binzel, 2002). The spectral classification is a key parameter enabling a preliminary assessment of possible composition, and consequently resources.

The taxonomic information from the SMASSII system is available for 313 NEAs, and used here as the baseline classification. The data set is completed by Tholen classes for 13 objects, with associated C and S groups to the corresponding classes of SMASSII system. The distribution of taxonomic types among the selected for the analysis asteroids is shown on Fig. 1. The most common is the S-complex of silicaceous (stony) asteroids, including the plain S-type, transitional sub-classes (Sa, Sq, Sr, Sk, and Sl) and A, K, L, Q, and R types. This group of objects consists mainly on iron- and magnesium-silicates. The X-type asteroids, constitute 15% of the sampling. This group includes Tholen E, M, and P-types. E-type is related to enstatite chondrite, while P-type to interplanetary dust particles (IDPs) bodies (Vernazza et al., 2015). M-type is mostly related to iron meteorites. However, not all objects are metallic: some of the M asteroids don't have a high radar albedo, nor high density (Ockert-Bell et al., 2010), and some present 3μ absorption tracking hydration (Rivkin et al., 2000). The C-group (carbonaceous) contains plain C-type and C sub-classes and B-type asteroids, forming around 8% of considered asteroids. Spectral features of each class are described in detail in (Bus and Binzel, 2002).

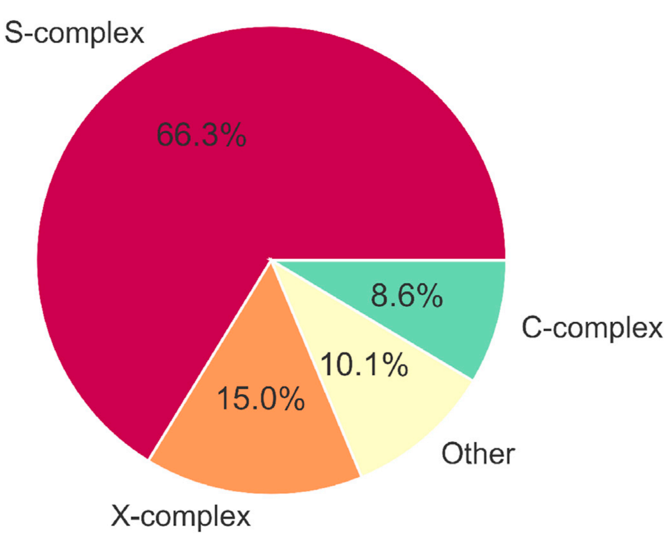

Fig. 1. Asteroid spectral classes. S-complex denotes Sa, Sq, Sr, Sk, and Sl transition classes between plain the S-type and the S-group classes. S-group denotes A, K, L, Q and R classes. C-group includes C- and B-types.

3. Compositional estimation

The vast majority of meteorites is originated from asteroids, providing a unique information about parent bodies. Dynamical models of the Solar System show that most of meteorites were transferred to near-Earth region from the main asteroid belt after entering in mean-motion or secular resonances (Granvik and Brown, 2018). Various meteorite-asteroid linkages have been proposed, connecting meteorite types to specific asteroid spectral classes (Cloutis et al., 2014).

The compositional interpretation from taxonomic types of asteroids and the links with meteorites is an inverse problem, and may involve ambiguities. The meteorite-asteroid linkages are usually not very certain due to non-unique spectra of asteroids' surfaces. Hence, different meteorite types may be linked to the same spectral class of asteroids. Table 1 summarises linkages of asteroid classes and possible meteorite analogs. This information is combined from McSween and Huss (2010), Binzel et al. (2019), Greenwood et al. (2020) and adopted in this work as input data. Then, chemical compositions of meteorites are adopted from McSween and Huss (2010) and assigned as an estimated composition to each asteroid.

3.1. S-complex asteroids

The S-complex of asteroids takes most of the data set: 214 objects, namely 66%.

The A-type of S-complex can be linked to pallasites or branchinites, which are likely to be samples of the same core as IIAB iron meteorites (Haack and McCoy, 2004), and consequently, we assume, have the same composition. The K-type can be linked to carbonaceous chondrites (CV and CO), and the L-type is associated to CAI-rich (rich in

Table 1
Meteorite types linkages for different asteroid taxonomic classes. The table compiles data from McSween and Huss (2010), Vernazza et al. (2015), Binzel et al. (2019), Greenwood et al. (2020).

Group	Spectral class SMASSII (Bus and Binzel, 2002)	Possible meteorite analogs
S-complex	A	pallasites, brachinites
	K	CV, CO, C3-ung.
	L, Ld	CAI-rich[a]
	S, Q, R, Sa, Sk, Sl, Sq, Sr	OC[b], PA[c], achondrites
C-complex	C, Cb, Cg, Ch, B	CM, CI, urelites, CR, K
X-complex	Xe	aubrites
	X, Xk, Xc	M, EH[d]
Other	D, T	C2-ung., IDPs[e]
	O	L or LL
	V	HED[f]

[a] Rich in Calcium-aluminium inclusions (CAI-rich).
[b] Ordinary chondrites (OC) include L, LL, H.
[c] Primitive achondrites (PA) and achondrites include angrites, acapulcoites-lodranites, winonaites, ureilites.
[d] Enstatite chondrites (EH).
[e] Interplanetary dust particles (IDPs).
[f] Howardite–eucrite–diogenite (HED).

Calcium-aluminium inclusions) meteorites which abundance increases from CO to CV (McSween and Huss, 2010).

The sample from Dunn et al. (2013) has S-type (including sub-types), Q- and K-types and a few V- and O-types, and crosses with 45 asteroids from our data set. We link other objects in the S-complex to ordinary chondrites meteorites, according to thr results from Itokawa and Hayabusa-1 missions (Binzel et al., 2004; Nakamura et al., 2011). For these objects, we set the estimated composition as the average between H, L and LL types.

3.2. Other spectral types of asteroids

Using the Bus and Binzel (2002) taxonomy, the C-complex asteroids are probably hydrated carbonaceous chondrites (e.g. CI or CM). The average chemical compositions of CI and CM chondrites is provided by McSween and Huss (2010), and shows a high presence of Fe, Si and Mg elements. The CI and CM chondrites are also more oxidized than other chondrites with about 44 wt% of oxigen in chemical composition.

The X-complex includes objects with spectra close to that of enstatite chondrites, aubrites, and iron types of meteorites. Besides a few objects from Dunn et al. (2013), which showed a resemblance with ordinary and carbonaceous chondrites, in this work we adopt the composition averaged by major iron meteorite groups from Haack and McCoy (2004).

The D- and T-class are associated with the C2-ungrouped, for which we use the averaged composition of hydrous carbonaceous chondrites CM, CR (Howard et al., 2015), containing about 18 wt% of water. The O-type is a rare spectral class, matching to the spectra of L and LL ordinary chondrite meteorites (Bus and Binzel, 2002). The V-type asteroids have a unique spectra and suggest a more definitive connections, such as between the asteroid Vesta and HED meteorites. The two unclassified asteroids, U-type, in our data-set for simplicity were also connected to HED meteorites accordingly to Chapman et al. (1978) and albedo values.

4. Trajectories database

The ECOCEL database ecocel-database.com holds trajectories for two classes of missions: one-way (Earth-to-asteroid) and round-trip (Earth-asteroid-Earth) missions, and collects 20 solutions of each class for each asteroid. The mission analysis for each asteroid in the database was performed for mission opportunities over 2025–2050 launch period. The computed trajectories in the database were found with the approximations listed below.

4.1. Methods, approximations and limitations

Constraints and parameters, listed below, are also summarised in Table 2.

Ephemerides. The ephemeris of Earth and asteroids were provided by the SPICE kernel files of the NAIF service (Annex et al., 2020; Acton, 1996).

Two-body approximation. Lambert's problem solver was used to find impulsive heliocentric transfer trajectory between Earth and asteroids with the optimal transfer segment that makes up to two revolutions around the Sun.

Sampling of parameters. Launch dates and mission duration form a discrete time space. For the one-way missions, the launch date and the time of flight were varied with 8-days and 10-days steps respectively. For the round-trip missions, the departure from Earth, the inbound and outbound times of flights, and the departure from asteroid were varied, and combined according to constraints on the total mission duration and the stay on asteroid. The trajectories were computed with 10-days steps for departure dates and 15-days steps of duration of inbound and outbound paths.

Launch window. The trajectories were computed for possible departure from 2025 01-01 to 2050-01-01.

Mission duration. The solutions stored in the database were computed for maximal duration of 450 days.

Stay at NEA (for round-trip missions only). The minimal stay at asteroid was set to 8 days.

Optimal solutions. The database collects 20 best solutions, minimised by the sum of departure and arrival v_∞, the hyperbolic excess velocities with respect to departure and arrival bodies, respectively.

Patched-conics. The database also provides the delta-V manoeuvres cost for a launch from a parking low Earth orbit (LEO), a 400 km altitude circular orbit. Another additional manoeuvre is for an Earth atmospheric entry, required when the spacecraft's speed at Earth arrival is more than 12 km/s at an altitude of 125 km. These delta-V calculations use the two-body patched conics approximation, and detailed below.

Table 2
Constraints and parameters for trajectories search.

Parameter	Value	
	One-way	Round-trip
Earth launch window	Jan 1, 2025 to Jan 1, 2050	
Launch date step	8 days	10 days
Mission duration	450 days	450 days
Time of flight step	10 days	15 days
Stay at NEA		≥8 days
Constraints for optional calculations		
Departure parking LEO altitude	400 km	400 km
Maximal Earth atmospheric re-entry velocity		12 km/s

4.2. Computation of manoeuvres

As pointed in the approximations for the trajectory search, the Lambert's problem solver was used for the discrete grid formed by launch dates and mission duration. The Lambert's problem solutions provide the required velocity change at a given moment to insert the spacecraft into the heliocentric transfer from Earth to NEA, or from NEA to Earth. Namely, this solution provides the hyperbolic excess velocity v_∞ at departure and arrival to the celestial body - Earth or asteroid. The trajectories, stored in the database, were optimized by the sum of four v_∞: velocities at departure from Earth, at arrival to asteroid, at departure from the asteroid and at arrival to Earth. In addition, the manoeuvres for the departure from a parking orbit and at the atmospheric re-entry are provided in the ECOCEL tool. These values are computed from the obtained values of excess velocities.

Earth departure. The hyperbolic excess velocity vector on exiting the Earth's sphere of influence (SOI) can be expressed as: $v_\infty = v_{sc} - v_E$ where v_{sc} and v_E are the velocities of the spacecraft and the Earth relative to the Sun. Namely, v_{sc} is the velocity that the spacecraft has to have to reach the asteroid, and can be found from the solution of Lambert's problem.

Let the trajectory design assume a departure from a parking 400 km altitude LEO. The delta-V of the insertion into the interplanetary orbit from the parking orbit can be computed as the difference between the velocity needed at the perigee to join a hyperbola with the required v_∞, $\sqrt{\frac{2\,\mu}{r_p} + v_\infty^2}$, (Bowell et al., 1989) and the velocity of the spacecraft on the parking orbit, $\sqrt{\frac{\mu}{r_p}}$. Hence, this manoeuvre is computed as: $\Delta v_1 = \sqrt{\frac{2\,\mu}{r_p} + v_\infty^2} - \sqrt{\frac{\mu}{r_p}}$, where r_p is the radius of the parking LEO, namely $R_E +$ 400 km where R_E is the radius of Earth; μ is the Earth's gravitational parameter (the constants are from the NAIF service (Annex et al., 2020)).

Asteroid arrival and departure. The delta-V of rendezvous corresponds to the maneuver required for the spacecraft to match the asteroid's speed and direction, and is calculated as the difference between velocity vectors of two objects. Namely, it is the hyperbolic excess velocity of the spacecraft $v_\infty = v_{sc} - v_{NEA}$, where v_{sc} and v_{NEA} are the asteroid's velocities relative to the Sun, and are obtained from the Lambert's problem solution. The maneuver to depart the NEA is estimated similarly:

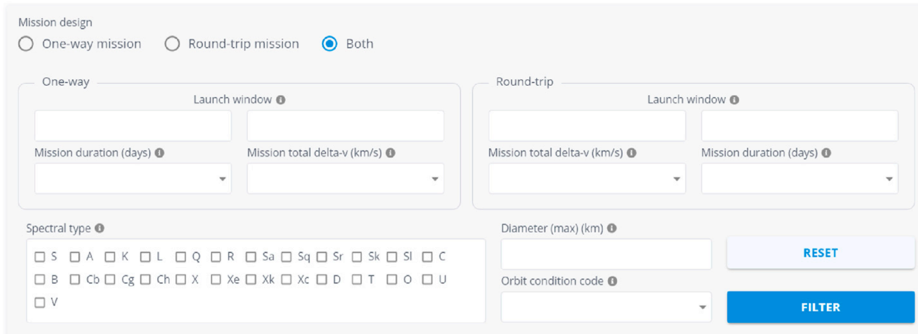

Fig. 2. Mission constraints form.

$$\Delta v_{arr} = v_\infty^-, \; \Delta v_{dep} = v_\infty^+ \qquad (1)$$

where v_∞^- and v_∞^+ are asteroid hyperbolic arrival and departure manoeuvres, respectively.

Earth arrival. Returning to Earth, the spacecraft with mined resources or attached to an entire asteroid can be repatriated into an orbit in cis-lunar space. To minimise the manoeuvre required for capturing into a bounded orbit the asteroid-spacecraft system should have the velocity at the sphere of influence (SOI) of Earth as low as possible.

In the case of asteroidal sample return to Earth, in order to prevent the capsule from destruction by the atmospheric drag, the allowed atmospheric entry speed may be limited by technical constraints. In the ECOCEL tool, this speed is arbitrary limited at 12 km/s at the altitude of 125 km, and a manoeuvre to fulfill this condition is computed, using the following formula:

$$\Delta v_2 = \sqrt{\frac{2\,\mu}{r_2} + v_\infty^2} - v_{limit}, \qquad (2)$$

where r_2 is $R_E + 125$ km and $v_{limit} = 12$ km/s.

5. Interface of online tool

The ecocel-database.com web-application is a tool that allows a user to find mission opportunities to asteroids within specific constraints.

5.1. Mission opportunities search

The mission constraints form (Fig. 2) allows users to specify the mission type - one-way or round-trip, or to enable both types. A user can set the acceptable launch windows from 2025 to 2050. The user can then constrain the mission duration and the total delta-V. Next, the parameters of suitable target asteroids can be specified: spectral types, diameter and orbit condition code. This last parameter is provided by JPL Small-Body Database (Chamberlin et al., 2020) and classifies the accuracy of asteroid's orbit resolution.

The specification of all the parameters is optional, and allows users to filter the solutions available in the database. If the parameters are not specified, all the mission opportunities are displayed. The solutions are then displayed in a table, which can be downloaded on .pdf and .csv formats. For each object, only one solution, which meets given constraints and corresponds to the minimal delta-V option, from the database is shown in the resulting table.

5.2. Target selection

A target asteroid available in the database can be chosen on a dedicated to search by asteroid's name or designation tool *Asteroids*. Alternatively, from the list of objects that were found to meet the user's mission constraints, any specific asteroid can also be selected to display further details in a separate page. This page provides additional information about the selected target asteroid, such as its name (if applicable), spectral type from the JPL Small Body Database (Chamberlin et al., 2020) and estimated diameter, also from the JPL Small Body Database or computed as described in 5.3.2. The page also contains an estimated composition of the target asteroid, derived from a linked meteorite type (Binzel et al., 2019; McSween and Huss, 2010) (Fig. 3).

For the selected target asteroid and corresponding to user's constraints, if there any, two solutions are summarised in the tables for one-way (Earth-to-asteroid) and round-trip (Earth-asteroid-Earth) trajectories. The table of one-way rendezvous mission contains the following parameters: departure from Earth and arrival to asteroid dates, time of flight, Earth departure v_∞, LEO departure delta-V, asteroid arrival delta-V and the total mission delta-V. The table of round-trip rendezvous mission contains the same parameters, and additionally: duration of stay on NEA, time of inbound flight, delta-V to depart NEA, Earth arrival v_∞, and the delta-V at Earth's atmosphere re-entry (if required).

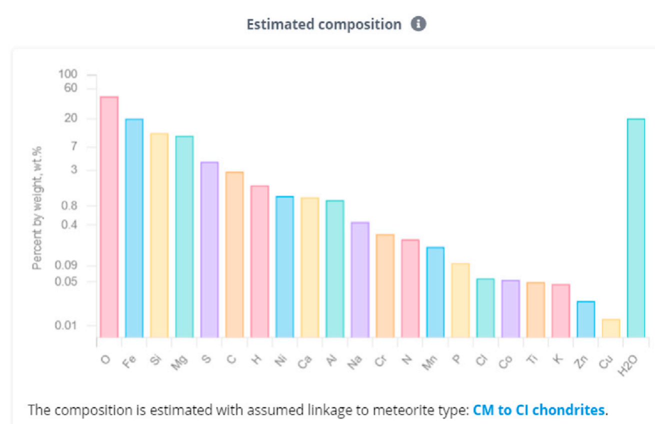

Fig. 3. Example of Bennu asteroid's estimated composition.

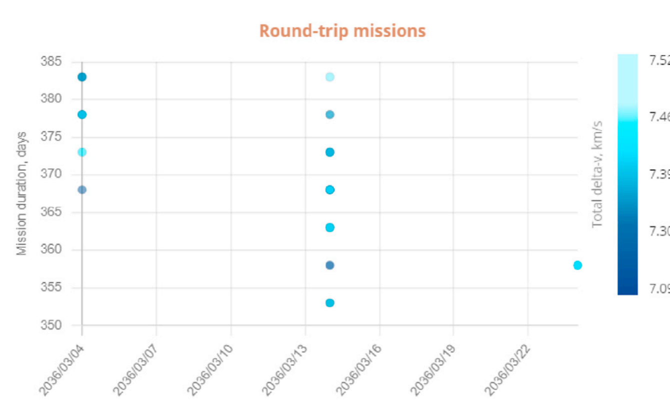

Fig. 4. Example of available round-trip solutions in the database.

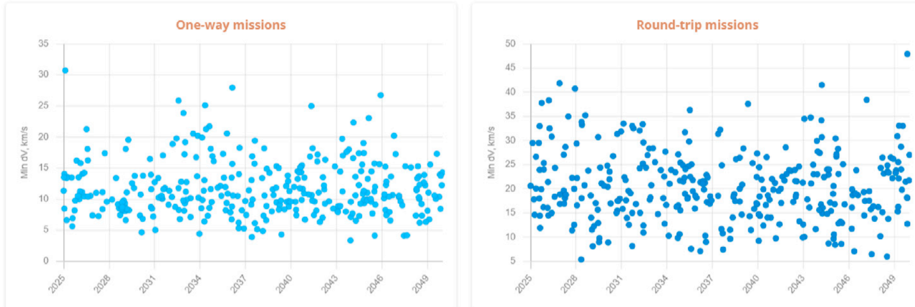

Fig. 5. Distribution of minimal delta-V values over 2020–2050 launch period.

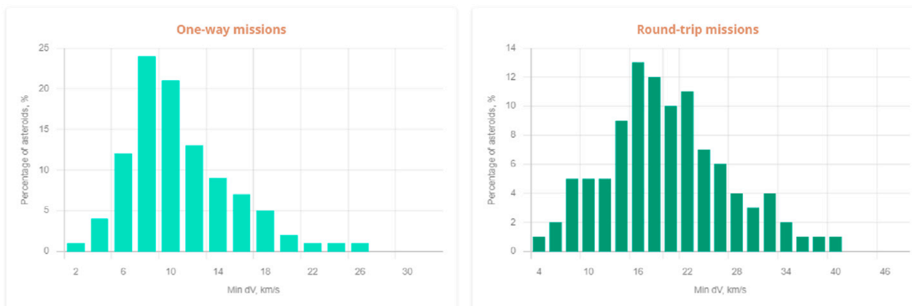

Fig. 6. Distribution of minimal delta-V values for the sample of 326 NEAs.

Besides the provided solution, two displayed plots provide all the 20 solutions stored in the database for both one-way and round-trip missions (example on Fig. 4).

5.3. Data analysis

The ECOCEL web-application includes *Data analysis* page, dedicated for a visualisation of data about accessibility and composition of potential targets.

5.3.1. Mission opportunities

The mission opportunities from the database are shown on diagrams of minimal delta-V values for each asteroid over 2020–2050 launch period (see Fig. 5). Fig. 6 shows the distribution of minimal delta-v values for the sample of 326 asteroids from the database.

5.3.2. Diameter distribution

Diameter of asteroids in the database is either provided by the JPL Small-Body Database or estimated from the absolute magnitude and average albedo values by the following formula [37]:

$$D = \frac{1329}{\sqrt{p_V}} 10^{-0.2H} \tag{3}$$

where H is asteroid's absolute magnitude and p_V is geometric albedo. This expression assumes the asteroid is a spherical object, with possible albedo range from 0.15 to 0.03. This rough estimation of the diameter is provided in the database table. For the visualisation of the diameter distribution (see Fig. 7) the mean value from the possible diameter's range was used.

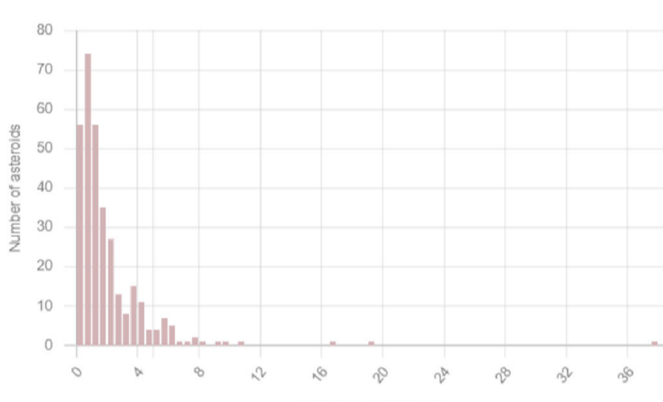

Fig. 7. Diameter distribution for the sample of 326 NEAs.

5.3.3. Compositional analysis

The ECOCEL web-application includes a visualisation of distribution of asteroids, containing a specific possible resource, as a function of

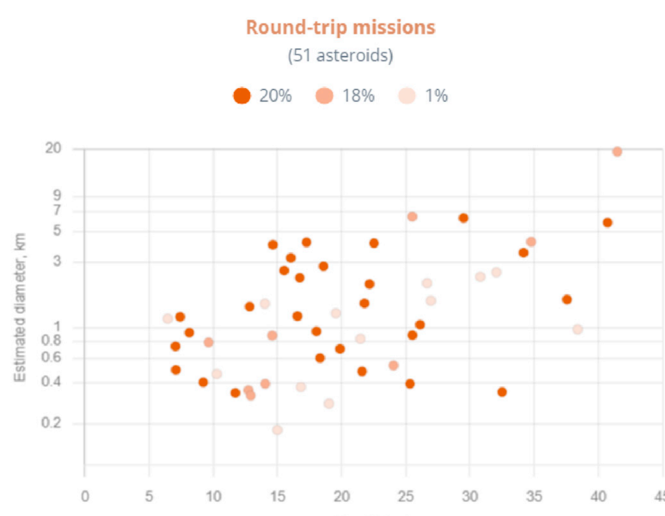

Fig. 8. Asteroids containing water. Distribution according to diameter and delta-v for round-trip rendezvous missions.

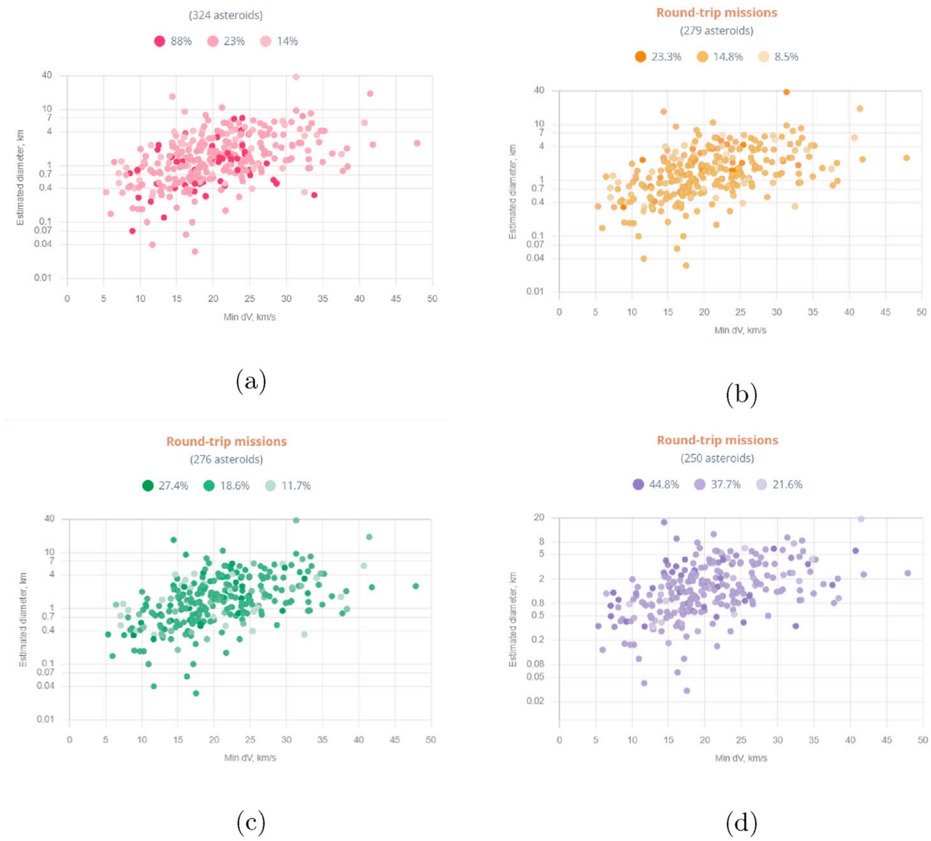

Fig. 9. Asteroids containing Fe (a), Mg (b), Si (c) and O (d). Distribution according to diameter and delta-v for round-trip rendezvous missions.

diameter and delta-V of the round-trip or one-way rendezvous missions. For instance, Fig. 8 shows the distribution of asteroids, with estimated water inclusions, and their accessibility expressed in delta-V values for round-trip missions. Fig. 9 shows asteroids containing iron, magnesium, silicon and oxygen.

6. Conclusions

The ECOCEL web-based tool ecocel-database.com is developed for a preliminary analysis of mission opportunities to asteroids. This paper describes the construction of the ECOCEL database, and the use of web-tools for searching and visualisation of required data.

First, the paper provides an overview of available asteroids in the database, their spectral classifications and explains the rough estimation of their composition. The compositional estimation is based on linkages of asteroids with meteorites. Then, the computation of mission parameters, including delta-v budget, mission duration, and optimal launch windows over 2025–2050 period is described. The transfer trajectories were found using two-body Lambert problem approximation and ephemerides of JPL HORIZONS system. The utilisation of the web-tool for searching transfer trajectories for one-way and round-trip rendezvous missions enables to introduce constraints on mission parameters and asteroid characteristics. Then, a suitable target asteroid can be selected for a detailed analysis of mission opportunities and chemical composition. Finally, a visualisation of potential resources, such as metals and volatiles, summarised for all asteroids in the database is presented.

The ECOCEL web-based tool allows to make preliminary mission target selection and provides an overview of a relatively small sample of asteroids, which is about 1% of the total NEAs population. In a future phase of the project, the database can be extended by additional sources of taxonomically classified asteroids, such as NEOSHIELD-2 (Perna et al., 2018), MANOS (Devogèle et al., 2019), and MITHNEOS (Binzel et al., 2019). In addition, a further mission design can be extended to a more complex analysis, including additional manoeuvres, gravity assists, implementation of low-thrust propulsion.

Declaration of competing interest

The authors declare that they have no known competing financial interests or personal relationships that could have appeared to influence the work reported in this paper.

References

Acton Jr., C.H., 1996. Ancillary data services of nasa's navigation and ancillary information facility. Planet. Space Sci. 44 (1), 65–70.

Annex, A.M., Pearson, B., Seignovert, B., Carcich, B.T., Eichhorn, H., Mapel, J.A., Von Forstner, J.L.F., McAuliffe, J., Del Rio, J.D., Berry, K.L., et al., 2020. Spiceypy: a pythonic wrapper for the spice toolkit. J. Open Source Software 5 (46), 2050.

Binzel, R.P., Perozzi, E., Rivkin, A.S., Rossi, A., Harris, A.W., Bus, S.J., Valsecchi, G.B., Slivan, S.M., 2004. Dynamical and compositional assessment of near-earth object mission targets. Meteoritics Planet Sci. 39 (3), 351–366.

Binzel, R., DeMeo, F., Turtelboom, E., Bus, S., Tokunaga, A., Burbine, T., Lantz, C., Polishook, D., Carry, B., Morbidelli, A., et al., 2019. Compositional distributions and evolutionary processes for the near-earth object population: results from the mit-Hawaii near-earth object spectroscopic survey (mithneos). Icarus 324, 41–76.

Bowell, E., Hapke, B., Domingue, D., Lumme, K., Peltoniemi, J., Harris, A.W., 1989. Application of photometric models to asteroids. Asteroids II, 524–556.

Bus, S.J., Binzel, R.P., 2002. Phase ii of the small main-belt asteroid spectroscopic survey: a feature-based taxonomy. Icarus 158 (1), 146–177.

Chamberlin, A., Yeomans, D., Giorgini, J., Chodas, P., 2020. Jet propulsion laboratory small-body database search engine. https://ssd.jpl.nasa.gov/sbdb_query.cgi.

Chapman, C.R., Williams, J.G., Hartmann, W.K., 1978. The asteroids. Annu. Rev. Astron. Astrophys. 16, 33–75.

Cloutis, E.A., Binzel, R.P., Gaffey, M.J., 2014. Establishing asteroid–meteorite links. Elements 10 (1), 25–30. https://doi.org/10.2113/gselements.10.1.25 arXiv: https://pubs.geoscienceworld.org/elements/article-pdf/10/1/25/3109422/25_v10n1.pdf.

Devogèle, M., Moskovitz, N., Thirouin, A., Gustaffson, A., Magnuson, M., Thomas, C., Willman, M., Christensen, E., Person, M., Binzel, R., et al., 2019. Visible spectroscopy from the mission accessible near-earth object survey (manos): taxonomic dependence on asteroid size. Astron. J. 158 (5), 196.

Dunn, T.L., Burbine, T.H., Bottke Jr., W.F., Clark, J.P., 2013. Mineralogies and source regions of near-earth asteroids. Icarus 222 (1), 273–282.
Elvis, M., McDowell, J., Hoffman, J.A., Binzel, R.P., 2011. Ultra-low delta-v objects and the human exploration of asteroids. Planet. Space Sci. 59 (13), 1408–1412.
Fujiwara, A., Kawaguchi, J., Yeomans, D., Abe, M., Mukai, T., Okada, T., Saito, J., Yano, H., Yoshikawa, M., Scheeres, D., et al., 2006. The rubble-pile asteroid itokawa as observed by hayabusa. Science 312 (5778), 1330–1334.
Granvik, M., Brown, P., 2018. Identification of meteorite source regions in the solar system. Icarus 311, 271–287.
Greenwood, R.C., Burbine, T.H., Franchi, I.A., 2020. Linking asteroids and meteorites to the primordial planetesimal population. Geochem. Cosmochim. Acta.
Haack, H., McCoy, T., 2004. Iron and Stony-Iron Meteorites. Treatise on Geochemistry, Meteorites, Comets and Planets, vol. 1.
Howard, K., Alexander, C.O., Schrader, D.L., Dyl, K., 2015. Classification of hydrous meteorites (cr, cm and c2 ungrouped) by phyllosilicate fraction: Psd-xrd modal mineralogy and planetesimal environments. Geochem. Cosmochim. Acta 149, 206–222.
Jedicke, R., Sercel, J., Gillis-Davis, J., Morenz, K.J., Gertsch, L., 2018. Availability and delta-v requirements for delivering water extracted from near-earth objects to cis-lunar space. Planet. Space Sci. 159, 28–42.
Lauretta, D., Balram-Knutson, S., Beshore, E., Boynton, W.V., d'Aubigny, C.D., DellaGiustina, D., Enos, H., Golish, D., Hergenrother, C., Howell, E., et al., 2017. Osiris-rex: sample return from asteroid (101955) bennu. Space Sci. Rev. 212 (1–2), 925–984.
McSween Jr., H.Y., Huss, G.R., 2010. Cosmochemistry. Cambridge University Press.
Nakamura, T., Noguchi, T., Tanaka, M., Zolensky, M.E., Kimura, M., Tsuchiyama, A., Nakato, A., Ogami, T., Ishida, H., Uesugi, M., et al., 2011. Itokawa dust particles: a direct link between s-type asteroids and ordinary chondrites. Science 333 (6046), 1113–1116.
J. NASA, 2020. Center for near-earth object studies. https://cneos.jpl.nasa.gov/.
NHATS, 2021. Accessible neas. https://cneos.jpl.nasa.gov/nhats/.
Ockert-Bell, M., Clark, B., Shepard, M., Isaacs, R., Cloutis, E., Fornasier, S., Bus, S., 2010. The composition of m-type asteroids: synthesis of spectroscopic and radar observations. Icarus 210 (2), 674–692.
Oleary, B., Gaffey, M.J., Ross, D.J., Salkeld, R., 1979. Retrieval of asteroidal materials. Space Resour. Space Settlements 173–189.
Perna, D., Barucci, M.A., Fulchignoni, M., Popescu, M., Belskaya, I., Fornasier, S., Doressoundiram, A., Lantz, C., Merlin, F., 2018. A spectroscopic survey of the small near-earth asteroid population: peculiar taxonomic distribution and phase reddening. Planet. Space Sci. 157, 82–95.
Probst, A., Nitzl, C., Kraus, F., Förstner, R., 2020. Cost estimation of an asteroid mining mission using partial least squares structural equation modelling (pls-sem). Acta Astronaut. 167, 440–454.
Rivkin, A., Howell, E., Lebofsky, L., Clark, B., Britt, D., 2000. The nature of m-class asteroids from 3-μm observations. Icarus 145 (2), 351–368.
Ross, S.D., 2001. Near-earth asteroid mining. Space 1–24.
Tholen, D., 1989. Asteroid taxonomic classifications. Asteroids.
Tsuda, Y., Saiki, T., Terui, F., Nakazawa, S., Yoshikawa, M., Watanabe, S.-i., Team, H.P., 2020. Hayabusa2 mission status: landing, roving and cratering on asteroid ryugu. Acta Astronaut. 171, 42–54.
Vernazza, P., Marsset, M., Beck, P., Binzel, R., Birlan, M., Brunetto, R., Demeo, F., Djouadi, Z., Dumas, C., Merouane, S., et al., 2015. Interplanetary dust particles as samples of icy asteroids. Astrophys. J. 806 (2), 204.
Veverka, J., Farquhar, B., Robinson, M., Thomas, P., Murchie, S., Harch, A., Antreasian, P., Chesley, S., Miller, J., Owen, W., et al., 2001. The landing of the near-shoemaker spacecraft on asteroid 433 eros. Nature 413 (6854), 390–393.
Webster, I., 2013. Asterank database. www.asterank.com.
Yárnoz, D.G., Sánchez, J.-P., McInnes, C.R., 2013. Easily retrievable objects among the neo population. Celestial Mech. Dyn. Astron. 116 (4), 367–388.
Zimmerman, D., Wagner, S., Wie, B., 2010. The first human asteroid mission: target selection and conceptual mission design. In: AIAA/AAS Astrodynamics Specialist Conference, p. 8370.